Mapana – Journal of Sciences
2025, Vol. 24, No. 2, *37-67*
ISSN 0975-3303|https://doi.org/10.12723/mjs.73.3

Synthesis, Characterization, In Silico ADME Profiling, MD Simulations and Unveiling Antibacterial Activities of Novel (E)-5-Amino-3-Styryl-1H-Pyrazole-4-Carbonitrile Derivatives: A Tandem Michael Addition Approach

Sivadharani P.* and Jayapradha S. R.*

Abstract

An easy and environment benign, time-efficient Tandem Michael addition for the synthesis of (E)-5-amino-3-styryl-1H-pyrazole-4-carbonitrile derivatives using the components of Cinnamaldehyde, hydrazine, and malononitrile through MCR approach have been developed. Using $AlCl_3$ as a catalyst in aqueous ethanol (1:1) medium, it yields 79–89% of the pyrazole derivative within the period of 30 minutes. The synthesised compounds were investigated for MM2 to predict the molecular behaviour and energy calculation by Chem 3D software, ADME (Adsorption, Distribution, Metabolism and Excretion) properties using Swiss ADME software to profile pharmacokinetic properties of potential drugs, and the compounds' molecular docking (MD) simulations procedure was done with the proteins 4O9I and 2HI9 Hydrolase inhibitors. The protein-ligand interactions between the synthesised compound and the chosen protein revealed antibacterial activity against gram positive and gram negative bacterium, with improved results shows the role of hydrolase inhibitors and their relevance in biological activity. These intriguing findings

* PG and Research Department of Chemistry, Government Arts College for Women, Nilakottai 624 208. Affiliated to Mother Teresa Women's University, Kodaikanal, India; *dharahavan823@gmail.com; https://orcid.org/0009-0008-8911-9943*; *srjayapradha2023@gmail.com, https://orcid.org/0009-0008-7427-9338*

indicate that the synthesized compounds might be suitable candidates for the development of novel antibacterial drugs in drug discovery.

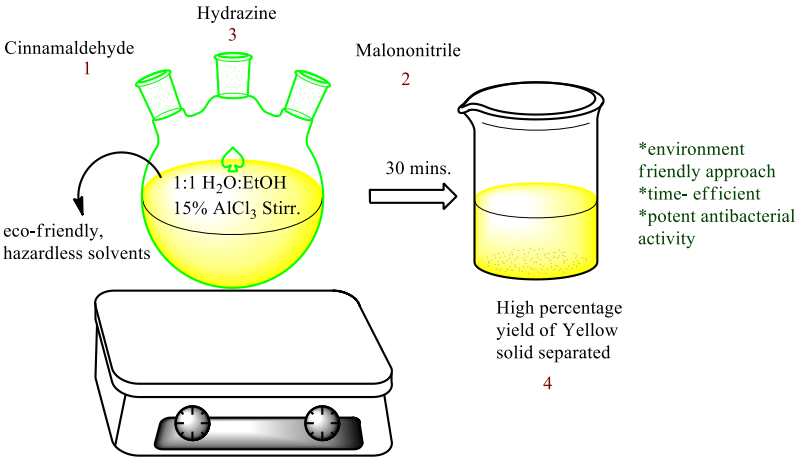

Graphical Abstract

Keywords: $AlCl_3$, Ethanol, MCR, Pyrazole, Tandem Michael addition, Water, ADME properties, MD simulations, Antibacterial activity.

1. Introduction

Multicomponent Reactions (MCR) brings together the greatest number of scientists and academics to expand a novel synthesis method for complex heterocyclic moiety. MCR has become a vital tool in synthetic organic chemistry, where three or more additives react within a single step to produce an excessively functionalized and complex product and also have biological significance [1, 2, 3]. Based on the principles of green chemistry, MCR reactions are now often employed to synthesise heterocyclic and organic molecules. MCRs have various advantages, including fewer reaction steps, increased efficiency, less purifying action, and cheaper costs. The reaction conditions, including appropriate solvents and catalysts, are crucial elements in MCR reactions[4]. It offers a quick and effective method to generate a variety of heterocycles with C-O and C-N linkages[5, 6]. Tandem Michael addition is a reaction between an α, β unsaturated carbonyl group (Michael acceptor) and a nucleophile (Michael donor) using a one-pot method[7]. A novel chemical framework, tandem Michael addition with formal isocyanide insertion into the acyl C-C bond, has been developed

recently[8]. Pyrazole, a five-membered ring with two nitrogen atoms, has become one of the most elegant N-heterocycles among other heterocyclic compounds. It exhibits a variety of organic and medicinal properties, such as anti-inflammatory, anti-cancer, anti-bacterial, anti-parasitic, anti-malarial, antitumor, antidepressant, analgesic and antiviral activities[9-13]. Numerous techniques for synthesising substituted pyrazole using various catalysts, including urea, trisodium citrate dehydrate, $ZnCl_2$ and $NaCNBH_3$, dodecylbenzene sulphonic acid, ZrO_2 nanoparticles, caesium fluoride, L-Proline, molecular I_2, K_2CO_3/glycerol, Mg-Fe hydrotalcite, $FeCl_3$/PVP, ionic liquid, and maltose, have been reported in the scientific literature [14-29].

This study reports on the hazard-free, time-efficient, environment-benign synthesis of pyrazole-based heterocyclic ring structures with a high yield of product using $AlCl_3$ as a catalyst and aims to synthesise several substituted 1H-pyrazole-4-carbonitrile derivative ring structures of extraordinary biological significance. The physiochemical properties, i.e., molecular formula, molar mass, water solubility, and number of H bond donors and acceptors, pharmacokinetic properties including GI (Gastro-intestinal) absorption, BBB (Blood brain barrier) permeation and Log Kp skin permeation, CYP1A2 and CYP2C19 inhibition activities, and drug-likeness assessment, including Lipinski, Ghose, Veber, Egan, and Muegge, show the importance of potential medications, which help in drug discovery, were observed. Two proteins were selected for docking; 2HI9 is a protein C inhibitor (PCI) and is a multifunctional serpin that has distinct cofactor-binding activities, a broad range of protease inhibitor activities, and perhaps non-inhibitory roles similar to those of hormone-transporting serpin. 4O9I, a new protein deposited in RSCB, helps in DNA binding. The interaction between these two proteins may provide crucial insights into their respective roles in cellular processes, and they both act as hydrolase inhibitors. The interaction between these two proteins may provide crucial insights into their respective roles in cellular processes, and they both act as hydrolase inhibitors. 2HI9 and 4O9I interact and could shed light on the mechanisms of protease regulation and the stabilisation of DNA structures, potentially revealing therapeutic approaches for related diseases. The MD simulations are carried out by the target compounds (synthesised ligand) with the two proteins 4O9I and 2HI9, which show antibacterial activity against the Gram-negative bacteria Escherichia coli such as Klebsiella oxytoca and Gram-positive bacteria such as Staphylococcus aureus and Staphylococcus epidermidis. These findings underscore the potential of these target compounds as promising candidates for developing new antibacterial therapies. Further exploration of their mechanisms of action

and optimisation could lead to effective treatments against resistant bacterial strains.

2. Experimental

2.1. Materials and Methods

The melting points have been determined in open capillaries using laboratory-grade chemicals and remained uncorrected. TLC was used to determine the purity of the chemical, UV-visible spectra were recorded, and IR spectra were recorded on an FT-IR using KBr. ^{1}H and ^{13}C NMR studies were recorded using Bruker 400 MHz for ^{1}H and 100 MHz for ^{13}C respectively. $AlCl_3$, Cinnamaldehyde, Malononitrile and Hydrazine all are readily available chemicals purchased from Nice brand and used without further purification.

2.2. General Procedure for Synthesis of (E)-5-amino-3-styryl-1H-pyrazole-4-carbonitrile (4a)

In a 250-mL round-bottom flask, cinnamaldehyde (10 mmol), malononitrile (10 mmol), 15% $AlCl_3$, and aqueous ethanol (1:1) were added, and the reaction mixture was refluxed by stirring. The progression of the reaction was observed by TLC. After the formation of an intermediate, 2 mmol of hydrazine was added. Once the reaction finished (as monitored by TLC), the reaction mixture was allowed to cool, the solid product was filtered off, rinsed with water, recrystallized it, and the melting points were recorded (**Scheme 1**).

2.3. Spectroscopic data of 1H and 13C NMR of the synthesized compounds

2.3.1. 4a (E)-5-amino-3-styryl-1H-pyrazole-4-carbonitrile

A combination of cinnamaldehyde (**1a**) (10 mmol), malononitrile (**2**) (10 mmol), 15% $AlCl_3$, and aqueous ethanol (1:1) was refluxed until the intermediate was produced, as determined by TLC. After the intermediate had formed, 2 mmol of hydrazine (**3**) was added. TLC verified the reaction's completion, after which the liquid was cooled, solid filtered, and recrystallized. Brown solid, m.p. 108 °C, Yield 89 %.

^{1}H NMR: δ 9.70 (1H, s), 6.50 (2H, s), 7.08 (1H, d, *J* = 14.0 Hz), 7.28-7.48 (6H, 7.34 (tt, *J* = 7.8, 1.4 Hz), 7.35 (tdd, *J* = 7.8, 1.6, 0.5 Hz), 7.38 (dddd, *J* = 7.8, 1.7, 1.4, 0.5 Hz), 7.41 (d, *J* = 14.0 Hz)).

^{13}C NMR: δ 108.9-109.0 (2C, 108.9 (s), 109.0 (s)), 114.6 (1C, s), 127.0 (1C, s), 127.3 (2C, s), 128.0-128.3 (2C, 128.1 (s), 128.2 (s)), 128.6 (2C, s), 134.8 (1C, s), 152.3 (1C, s).

2.3.2. 4b (E)-5-amino-3-(4-chlorostyryl)-1H-pyrazole-4-carbonitrile

A combination of substituted 4-chlorocinnamaldehyde (**1b**) (10 mmol), malononitrile (**2**) (10 mmol), 15% $AlCl_3$, and aqueous ethanol (1:1) was refluxed until the intermediate was produced, as determined by TLC. After the intermediate had formed, 2 mmol of hydrazine (**3**) was added. TLC verified the reaction's completion, after which the liquid was cooled, solid filtered, and recrystallised. Brown solid, m.p. 219°C, Yield 85%

^{1}H NMR: δ 9.72 (1H, s), 6.53 (2H, s), 7.06 (1H, d, *J* = 14.0 Hz), 7.19-7.41 (5H, 7.25 (ddd, *J* = 7.9, 1.5, 0.5 Hz), 7.31 (ddd, *J* = 7.9, 1.7, 0.5 Hz), 7.35 (d, *J* = 14.0 Hz)).

^{13}C NMR: δ 108.9-109.0 (2C, 108.9 (s), 109.0 (s)), 114.6 (1C, s), 127.0 (1C, s), 128.1-128.4 (3C, 128.2 (s), 128.3 (s)), 128.9 (2C, s), 134.1 (1C, s), 134.8 (1C, s), 152.3 (1C, s).

2.3.3. 4c (E)-5-amino-3-(2-nitrostyryl)-1H-pyrazole-4-carbonitrile

A combination of 2-nitrocinnamaldehyde (**1c**) (10 mmol), malononitrile (**2**) (10 mmol), 15% $AlCl_3$, and aqueous ethanol (1:1) was refluxed until the intermediate was produced, as determined by TLC. After the intermediate had formed, 2 mmol of hydrazine (**3**) was added. TLC verified the reaction's completion, after which the liquid was cooled, solid filtered, and recrystallised. Yellow solid, m.p. 173°C, Yield 83%

^{1}H NMR: δ 9.75 (1H, s), 6.54 (2H, s),7.36 (1H, d, *J* = 15.6 Hz), 7.57 (1H, ddd, *J* = 8.6, 7.7, 1.4 Hz), 7.66-7.81 (2H, 7.74 (ddd, *J* = 7.7, 7.3, 1.8 Hz), 7.75 (ddd, *J* = 7.3, 1.4, 0.5 Hz)), 8.03 (1H, d, *J* = 15.6 Hz), 8.29 (1H, ddd, *J* = 8.6, 1.8, 0.5 Hz).

^{13}C NMR: δ 108.9-109.0 (2C, 108.9 (s), 109.0 (s)), 114.6 (1C, s), 124.9 (1C, s), 125.0 (1C, s), 128.1-128.4 (2C, 128.2 (s), 128.3 (s)), 128.5-128.7 (2C, 128.6 (s), 128.6 (s)), 132.5 (1C, s), 148.0 (1C, s), 152.3 (1C, s).

2.3.4. 4d (E)-5-amino-3-(2-hydroxystyryl)-1H-pyrazole-4-carbonitrile

A combination of 2-hydroxycinnamaldehyde (**1d**) (10 mmol), malononitrile (**2**) (10 mmol), 15% $AlCl_3$, and aqueous ethanol (1:1) was refluxed until the intermediate was produced, as determined by TLC. After the intermediate had formed, 2 mmol of hydrazine (**3**) was added. TLC

verified the reaction's completion, after which the liquid was cooled, solid filtered, and recrystallised. Yellow solid, m.p. 110 °C, Yield 85 %

^{1}H NMR: 9.78 (1H, s), 6.53 (2H, s)δ 6.96-7.38 (5H, 7.03 (d, *J* = 15.9 Hz), 7.08 (ddd, *J* = 8.0, 1.4, 0.5 Hz), 7.13 (ddd, *J* = 7.4, 7.2, 1.4 Hz), 7.20 (ddd, *J* = 8.0, 7.4, 1.4 Hz), 7.31 (d, *J* = 15.9 Hz)), 7.44 (1H, ddd, *J* = 7.2, 1.4, 0.5 Hz).

^{13}C NMR: δ 108.9-109.0 (2C, 108.9 (s), 109.0 (s)), 114.6 (1C, s), 116.5 (1C, s), 121.0 (1C, s), 125.0 (1C, s), 128.1-128.4 (2C, 128.2 (s), 128.3 (s)), 128.5-128.7 (2C, 128.6 (s), 128.6 (s)), 152.3 (1C, s), 160.0 (1C, s).

2.3.5. 4e (E)-5-amino-3-(2-bromostyryl)-1H-pyrazole-4-carbonitrile

A combination of 2-bromocinnamaldehyde (**1e**) (10 mmol), malononitrile (**2**) (10 mmol), 15% $AlCl_3$, and aqueous ethanol (1:1) was refluxed until the intermediate was produced, as determined by TLC. After the intermediate had formed, 2 mmol of hydrazine (**3**) was added. TLC verified the reaction's completion, after which the liquid was cooled, solid filtered, and recrystallised. Pale yellow solid, m.p. 83 °C, Yield 87 %

^{1}H NMR: δ 9.72 (1H, s), 6.57 (2H, s)6.87-7.16 (3H, 6.94 (ddd, *J* = 7.9, 7.3, 1.8 Hz), 7.05 (d, *J* = 15.5 Hz), 7.10 (ddd, *J* = 8.3, 1.8, 0.6 Hz)), 7.19-7.43 (3H, 7.26 (ddd, *J* = 7.9, 1.4, 0.6 Hz), 7.29 (ddd, *J* = 8.3, 7.3, 1.4 Hz), 7.36 (d, *J* = 15.5 Hz)).

^{13}C NMR: δ 108.9-109.0 (2C, 108.9 (s), 109.0 (s)), 114.6 (1C, s), 123.5 (1C, s), 125.0 (1C, s), 128.1-128.4 (2C, 128.2 (s), 128.3 (s)), 128.5-128.7 (2C, 128.6 (s), 128.6 (s)), 133.0 (1C, s), 136.3 (1C, s), 152.3 (1C, s).

3. Results and Discussion

The synthesis of pyrazole-4-carbonitrile derivatives in aqueous media with CuO/ZrO_2 as recyclable catalyst, an eco-friendly approach has been reported recently by S Maddila and co-workers[30]. The high percentage of yield was obtained within the short time of duration. Likewise, it has been planned to synthesize environment benign pyrazole derivatives using $AlCl_3$ as a catalyst. The readily available chemical aluminium chloride chosen here serves as a Lewis acid catalyst, facilitating the reaction between reactants and thereby increasing reaction rates. This catalytic effect can significantly enhance yields and reduce reaction times, making it a valuable compound in various chemical syntheses. Its ability to form complexes with electron donors enhances its catalytic effectiveness in organic transformations.

The Present work investigates the reaction of Cinnamaldehyde (**1**), malononitrile (**2**), hydrazine (**3**) with $AlCl_3$ catalyst and 1:1 of harmless eco eco-friendly solvents of EtOH and water medium. In a solvent mixture of

ethanol and water (1:1, v/v), the best outcome is achieved with a catalyst of 15 mol% $AlCl_3$. The reaction is continued until the yellow precipitate is obtained. The reaction is run for 1 hour, 30 minutes, and 45- minutes to check for the reaction's completion and yield and to improve the reaction time. After 30 minutes of the response, the final product doesn't change. The addition of all the reactants simultaneously gives the product of 40% yield. So, the reaction is carried out step-by-step to avoid the low percentage of yield.

Cinnamaldehyde (**1**), a flavouring agent which is obtained from cinnamon, carries an α, β-unsaturated group chosen here as an aldehyde to promote the reaction with malononitrile and hydrazine to give the desired products 4a-e with high percentage of yield (**Figure 2, Graph 1**).

Commonly Malononitrile (**2**) undergoes both 1,3 dipolar cycloaddition and nucleophilic addition reactions. In nucleophilic addition, it gives aminopyrazoles or hydrazides when it reacts with hydrazine[30]. The aldehyde chosen here was Cinnamaldehyde (**1**), which is an α, β unsaturated aldehyde and a trans isomer that exhibits pharmacological effects and neuro-protection properties. Due to α, β unsaturated aldehyde **1** (Cinnamaldehyde), there is a possible for 1,2 addition as well as 1,4 addition with malononitrile. Usually, soft nucleophiles undergo 1,2 addition and hard nucleophiles undergo 1,4 addition reaction. Malononitrile a soft nucleophile which undergo 1, 2 addition and 1, 4 addition is not possible here for the intermolecular cyclisation. The possible way to approach the product is only through 1,2 addition and not by 1,4 addition.

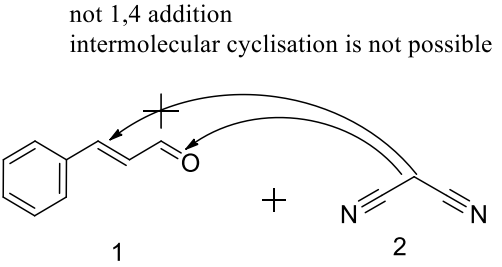

Figure 1: Possible addition in the reaction

The ^1H spectrum shows the peaks of NH broad singlet at δ 9.70 which confirms the cyclization of the product pyrazole, NH_2 singlet at δ 6.50, aldehyde CH doublet at δ 7.08, 6H aromatic multiplets at δ 7.28-7.48 region, Ar-H triplet of triplet at δ 7.34, Ar-H triplet of doublet of doublet at δ 7.35 , Ar-H doublet of doublet of doublet of doublet at δ 7.38 and another aldehyde CH doublet at δ 7.41ppm. In ^{13}C NMR, the Carbon attached with NH_2 group of the hydrazine gives peak at δ 152.3, the carbon attached with

malononitrile CN group and the carbon attached with the aldehyde group observed at δ 108.9 and δ 109 respectively and the malononitrile C at δ 114. The ^{13}C spectrum confirms the formation of the pyrazole ring derivatives. The UV absorption occurs at 379.50, 348.00, 261.50, 366.00, 291.50, 249.00 nm confirms the formation of the 1H pyrazole ring (**Figure 1**). And the FT-IR spectral information specified in (**Table 1**).

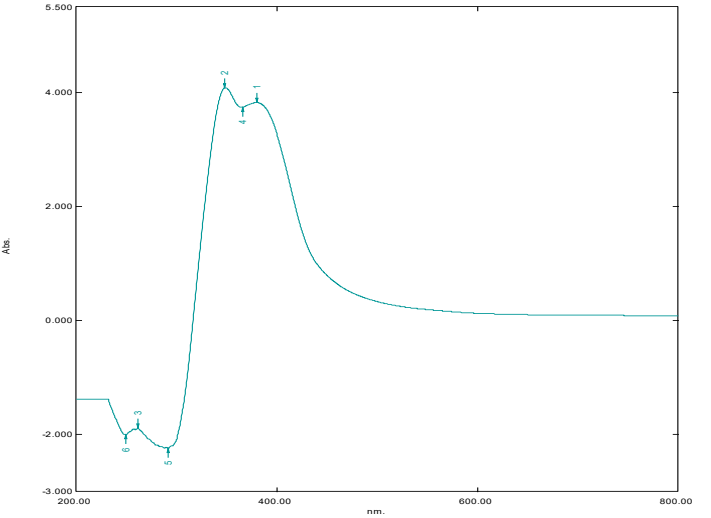

Figure 2: UV absorption of (E)-5-amino-3-styryl-1H-pyrazole-4-carbonitrile

Table 1: FT-IR range for the synthesized compounds 4a-e

Compound	NH Stretch (cm^{-1})	CN stretch (cm^{-1})	Aromatic and Pyrazole ring	
			CH aromatic Stretch (cm^{-1})	CC bends (cm^{-1})
4a	3346	2110	3053	1600
4b	3339	2018	3010	1609
4c	3330	2113	3022	1602
4d	3349	2120	3015	1615
4e	3341	2100	3034	1621

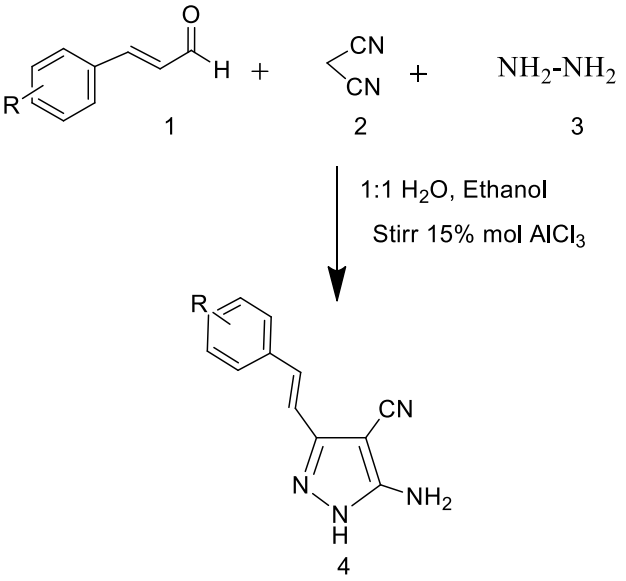

(*E*)-5-amino-3-styryl-1*H*-pyrazole-4-carbonitrile

Scheme 1

Table 2: Yield observed in the synthesized compounds 4a-e

Compound	R	Yield%
4a	H	89
4b	4-Cl	85
4c	2-NO_2	83
4d	2-OH	85
4e	2-Br	87

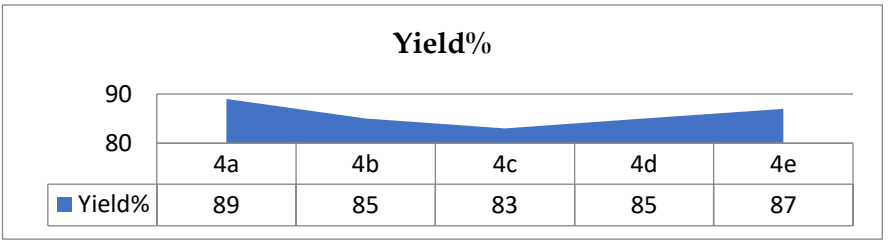

Graph 1: percentage of yield observed for the compounds 4a-4e

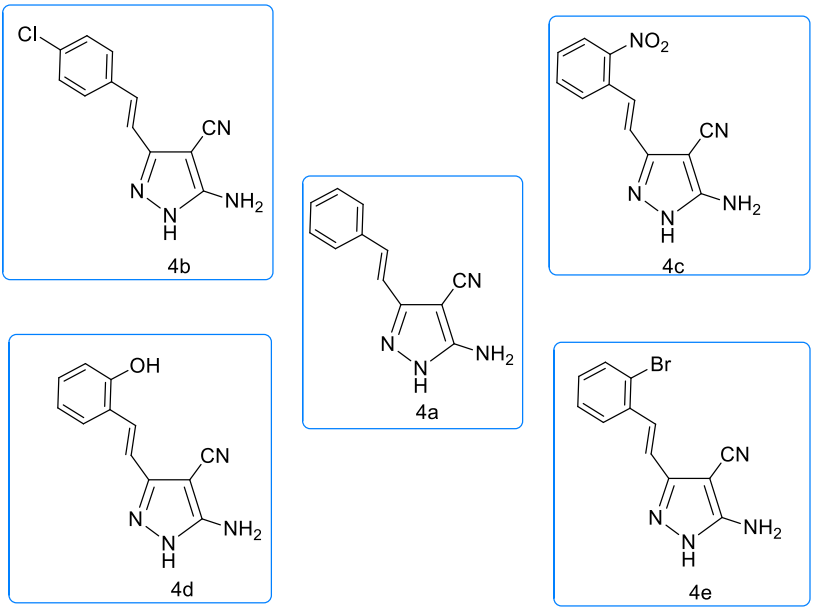

Figure 3: structure of the synthesized 1H-pyrazole carbonitrile derivatives 4a-e

3.1. The plausible mechanism of the reaction

The formation of (E)-5-amino-3-styryl-1H-pyrazole-4-carbonitrile (4a) was carried out by a Knoevenagel reaction followed by a Michael-type addition and intermolecular cyclization. Firstly, one of the most nucleophilic amino groups from the hydrazine is added to the cinnamaldehyde and malononitrile, resulting in the intermediate (E)-2-(1-hydrazinyl-3-phenylallyl) malononitrile, which undergoes elimination and rearrangement to give another intermediate, 2-((1Z,2E)-1-hydrazono-3-phenylallyl) malononitrile. This intermediate undergoes intramolecular cycloaddition through the nucleophilic attack of another amine group on the nitrile carbon, this cyclization results in the formation of a five-membered pyrazole ring, which is crucial for imparting biological activity to the final compound yielding (E)-5-imino-3-styryl-4,5-dihydro-1H-pyrazole-4-carbonitrile, a key functional group which further transformation leads to the product 4a, (E)-5-amino-3-styryl-1H-pyrazole-4-carbonitrile derivative

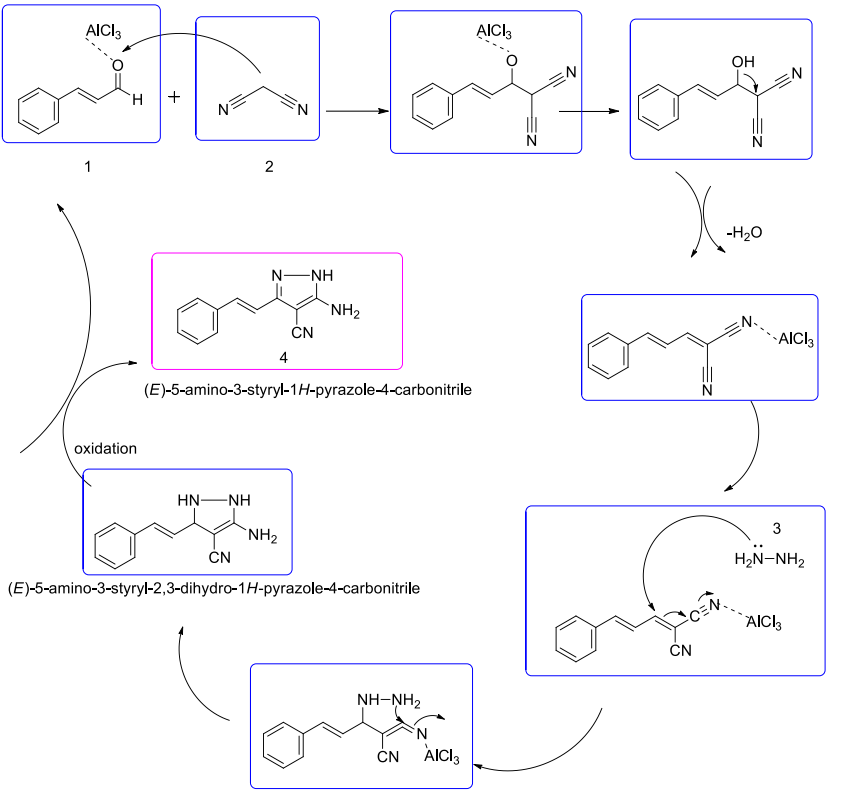

Figure 4: Structure of the synthesised 1H-pyrazole carbonitrile derivatives 4a-e

3.2. Computational Methods

Experimentation, while invaluable, can be time-consuming and costly, making computational methods an attractive option for rapidly predicting ADME properties. By leveraging advanced algorithms and large datasets, researchers can identify promising candidates and optimise their pharmacokinetic profiles before moving on to more resource-intensive experimental validation. Chemdraw and Chem3D software are used for the structure confirmation, stereochemistry and MM2 calculations.

3.2.1. ADME properties of all the synthesized compounds (4a-4e)

To be effective as a medicine, a powerful molecule must reach its target in the body in sufficient quantity and remain in a bioactive state long enough for the predicted biological activities to occur. Drug development involves

studying how a drug is absorbed, distributed, metabolised, and excreted early on when there are many potential compounds to consider, but only a few physical samples are available. In this sense, computer models are legitimate alternatives to experimentation. Here, the ADME properties can be determined using the open-source SwissADME, a free online tool that predicts physicochemical properties (**Table 3**), pharmacokinetics (**Table 4**) and drug-likeness (**Table 5**). The synthesised structure was drawn in the SwissADME portal. It was converted into SMILES. By clicking the run option, all the properties are observed. This information is crucial for understanding the compound's behaviour in biological systems and its suitability for further development.

Table 3: Physiochemical properties of 4a-e

Physiochemical properties	**4a**	**4b**	**4c**	**4d**	**4e**
Formula	C12H10N4	C12H9ClN4	C12H9N5O2	C12H10N4O	C12H9BrN4
Molecular weight	210.23 g/mol	244.68 g/mol	255.23 g/mol	226.23 g/mol	289.13 g/mol
Num. heavy atoms	16	17	19	17	17
Num. arom. heavy atoms	11	11	11	11	11
Fraction Csp3	0.00	0.00	0.00	0.00	0.00
Num. rotatable bonds	2	2	3	2	2
Num. H-bond acceptors	2	2	4	3	2
Num. H-bond donors	2	2	2	3	2
Molar Refractivity	63.08	68.09	71.90	65.10	70.78
TPSA	78.49 Å²	78.49 Å²	124.31 Å²	98.72 Å²	78.49 Å²
Log P	1.80	2.35	1.03	1.37	2.42
Water Solubility	Soluble	Moderately soluble	Soluble	Soluble	Moderately soluble

Table 4: Pharmacokinetics for the synthesized compounds 4a-e

Pharmacokinetics	**4a**	**4b**	**4c**	**4d**	**4e**
GI absorption	High	High	High	High	High
BBB permeant	No	No	No	No	Yes
P-gp substrate	No	No	No	No	No
CYP1A2 inhibitor	Yes	Yes	Yes	No	Yes
CYP2C19 inhibitor	No	Yes	No	No	Yes
CYP2C9 inhibitor	No	No	No	No	No
CYP2D6 inhibitor	No	No	No	No	No
CYP3A4 inhibitor	No	No	No	No	No
Log K_p (skin permeation)	-5.85 cm/s	-5.61 cm/s	-6.25 cm/s	-6.20 cm/s	-5.84 cm/s

From the ADME properties, the synthesised compounds 4a-e show high GI absorption (i.e., above 80 %; less than 30 % indicates poor absorption). These findings indicate that these molecules can be easily absorbed by the intestine and circulate in the bloodstream. With the exception of 4e, all synthesized compounds exhibit no permeability across the BBB. This suggests that compounds 4a, 4b, 4c, and 4d can achieve brain perfusion through direct injection into the carotid artery, resulting in systemic distribution effects that may alter brain penetration without impacting the central nervous system (CNS). The primary focus of phase I in drug discovery is the study of metabolizing enzymes. Among the ADME properties, Cytochrome P450 CYP1A2 is a human microsomal enzyme that plays a significant role in drug metabolism. All the synthesised compounds show activity against CYP1A2 except 4d. CYP2C19 inhibitor shows activity only in 4b and 4e. The lowest value of Log Kp (skin permeability) indicates a low probability of transdermal delivery.

Table 5: Druglikeness of 4a-e

Druglikeness	**4a**	**4b**	**4c**	**4d**	**4e**
Lipinski	Yes	Yes	Yes	Yes	Yes
Ghose	Yes	Yes	Yes	Yes	Yes
Veber	Yes	Yes	Yes	Yes	Yes
Egan	Yes	Yes	Yes	Yes	Yes

Muegge	Yes	Yes	Yes	Yes	Yes

All synthesized compounds (4a-e) strictly adhere to Lipinski's rule of five, which states that MW should be less than or equal to 500, log P should be less than or equal to 5, the number of H-bond donors should not exceed 5, and the number of H-bond acceptors should not exceed 10, along with a maximum of 10 rotatable bonds, indicating their drug-likeness and bioavailability score is 0.55 for all the synthesized compounds. Evaluating the bioavailability and drug-likeness of these compounds according to the established criteria of Lipinski, Ghose, Veber, Egan, and Muegge not only confirms their potential but also highlights their promise as suitable pharmaceutical candidates. The enhanced understanding of the pharmacokinetics and drug-likeness of pyranopyrazole derivatives, derived from in silico ADME predictions, opens avenues for further research and optimisation efforts. This knowledge could lead to the development of more effective therapeutic agents suited to specific diseases. Additionally, the integration of experimental validation will be crucial in confirming the predicted properties and ensuring their practical applicability in drug development.

In Chem3D, MM2 (molecular mechanics) computations are performed to optimise the exact arrangement (**Figure 3)**, shape and energy of molecules. This entails estimating the potential energy of the molecule based on its atomic interactions (bond lengths, bond angles, torsion angles, and van der Waals forces) and repeatedly altering the atomic locations to achieve a stable, low-energy conformation. Stereochemistry assigned as follows,

C(4): (S)

C(2)-C(3): (E)

C(9)-C(8): (E)

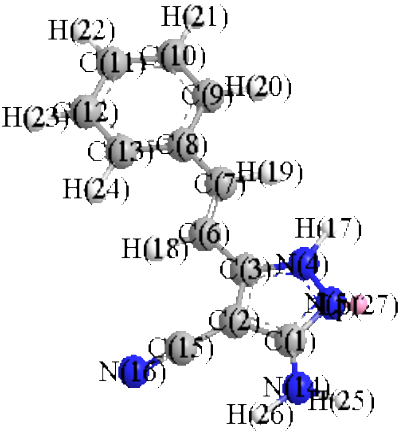

Figure 5: 3D model of pyrazole carbonitrile derivative 4a

MM2 Dynamics

There are three π systems observed in the synthesized compound between the following ring systems

π System: 10 8 9 20 21

π System: 17 16 3 2 15 1 18 19

π System: 11 5 6 12 13

The only accessible computational tools for molecular modelling are molecular mechanics and dynamics, both of which require accurate molecular parameters. Chemical intuition and trial-and-error procedures can provide appropriate parameters, but Chem 3D model simulations are the convenient method. This technique is more dependable and time-efficient than molecular dynamics for identifying all trustworthy minimums.

The newly derived parameters were utilised to simulate synthesised molecules, resulting in spectroscopically confirmed structures. Separate conformational searches were conducted for each instance. All the stretch, bend, force and dielectric constant are calculated. Cubic stretch constant - 2.000, Quartic stretch constant 2.333, X-B,C,N,O-Y Stretch-Bend interaction force constant 0.120, X-B,C,N,O-H Stretch-Bend interaction force constant 0.090 Sextic bending constant (* 10**8) 7.000, Dielectric constant for dipoles 1.500, Cutoff distance for charge/charge interactions 35.000, Cutoff distance for charge/dipole interactions 25.000, Cutoff distance for dipole/dipole interactions 18.000, Cutoff distance for van der Waals interactions 10.000 .

Table 6: The bond length, stretching and dipole charges of synthesised pyrazole

Bond	KS	Bond Length	Dipole
2-2	9.600	1.337	0.000
2-5	4.600	1.100	0.000
1-2	4.400	1.497	0.300
1-5	4.600	1.113	0.000
2-6	6.000	1.355	0.000
2-37	11.090	1.260	0.583
2-40	11.090	1.266	0.870
2-4	9.900	1.313	0.000

23-40	6.100	1.050	0.550
37-40	11.000	1.230	0.300
4-10	17.730	1.158	3.400

Table 7: The values for the three possible bending angles of KB: XR2, XRH, and XH2

Angle	KB	XR2	XRH	XH2
2-2-2	0.430	120.0	0.0	0.0
2-2-5	0.360	120.0	120.5	0.0
1-2-5	0.360	118.2	0.0	0.0
1-2-2	0.550	121.4	122.0	120.0
2-1-5	0.360	109.4	109.4	110.0
2-1-2	0.450	109.5	109.5	109.5
6-2-37	0.400	120.0	0.0	0.0
2-2-37	0.430	120.0	123.5	0.0
2-2-6	0.700	124.3	0.0	0.0
2-6-2	0.770	112.0	0.0	0.0
2-2-40	0.430	120.0	119.0	0.0
2-2-4	0.360	120.0	0.0	0.0
1-2-4	0.470	122.0	0.0	0.0
23-40-23	0.190	118.8	0.0	0.0
2-40-23	0.360	118.0	0.0	0.0
1-2-40	0.550	125.3	0.0	0.0
23-40-37	0.360	113.0	0.0	0.0
2-40-37	0.430	124.0	124.0	0.0
2-37-40	0.430	115.0	0.0	0.0
5-1-5	0.320	109.4	109.0	109.5
2-4-10	0.500	180.0	0.0	0.0

The employed technique provided a consistent set of parameters (**Table 6 & Table 7**). The calculated vibrational frequencies, however, make

it clear that quantum mechanical approaches typically overestimate the force constants. This impact was taken into consideration by downscaling the calculated stretching and bending constants. An analogy with the values already present in the MM2 force field was used to determine the bending constants involving lone pairs. Since the van der Waals and electrostatic contributions of lone pairs often constitute the most significant conformationally relevant characteristics, the torsional constants affecting lone pairs were set to 0.00. This approach ensures that the model remains computationally efficient while accurately capturing the essential interactions in the system. Consequently, the refined force field can better predict the molecular geometries and energy landscapes pertinent to the studied conformations.

Torsion angles/dihedral angles are essential for establishing a molecule's overall 3D structure and are employed in molecular mechanics calculations (**Table 8**).

Table 8: The Torsional angles V1, V2 and V3

Torsional	**V1**	**V2**	**V3**
2-2-2-5	0.000	9.000	-1.060
2-2-2-2	-0.930	8.000	0.000
5-2-2-5	0.000	15.000	0.000
1-2-2-5	0.000	12.500	0.000
1-2-2-2	-0.270	10.000	0.000
5-1-2-5	0.000	0.000	0.520
2-1-2-5	0.000	0.000	0.600
2-2-1-5	0.000	0.000	-0.240
2-1-2-2	0.100	0.000	0.500
4-2-1-5	0.000	0.000	-0.240
2-1-2-4	0.100	0.000	0.500
2-2-2-37	1.000	15.000	0.000
1-2-2-37	0.000	15.000	0.000
2-2-2-6	0.000	16.250	0.000
1-2-2-6	-1.200	16.250	0.000
1-2-2-1	-0.100	10.000	0.000

Torsional	V1	V2	V3
2-2-2-40	0.000	15.000	0.000
1-2-2-40	0.000	15.000	0.000
0-0-0-0	0.000	0.000	0.000
2-2-6-2	0.000	0.000	0.000
2-2-37-40	0.000	10.000	0.000
2-2-40-23	0.000	15.000	0.000
1-2-40-23	0.000	15.000	0.000
2-2-40-37	0.000	15.000	0.000
5-1-2-40	0.000	0.000	0.000
2-37-40-23	0.000	10.000	0.000
2-37-40-2	0.000	10.000	0.000

The atomic radius plays a vital role in guiding how atoms interact and bond with each other. The parameter known as Eps, or 'epsilon,' regulates the significance or influence of the atomic radius. In Chem3D, the 'weight' parameter designates the importance of a particular atomic radius in shaping the overall molecular geometry. The term 'Reduction' pertains to diminishing the influence of lone pairs on the three-dimensional structure of the molecule. While lone pairs affect the angles and connections between atoms, their influence must sometimes be adjusted or 'reduced.' Fine-tuning the 3D configuration of molecules in Chem3D involve modifying the effects of atomic radii, especially regarding the impact that lone pairs have on the molecular geometry (**Table 9**).

Table 9: The Atomic radii, Eps, Weight reduction and lone pair parameters of the synthesized 3D molecule

MM2	c3d	AtomRadius	Eps	Weight Reduction	Lone Pairs
2	1.940	0.044	12.000	0.000	0
1	1.900	0.044	12.000	0.000	0
6	1.740	0.050	15.995	0.000	2
40	1.820	0.055	14.003	0.000	0
37	1.820	0.055	14.003	0.000	1

MM2	c3d	AtomRadius	Eps	Weight Reduction	Lone Pairs
4	1.940	0.044	12.000	0.000	0
10	1.820	0.055	14.003	0.000	0
5	1.500	0.047	1.008	0.915	0
23	1.050	0.034	1.008	0.000	0

The configuration of electrons surrounding a central atom in a molecule, along with their three-dimensional shape, is regulated by the Valence Shell Electron Pair Repulsion (VSEPR) theory. The foundation of this theory is the idea that electron pairs surrounding a central atom—including bonded and lone pairs—repel one another and arrange themselves to lessen this repulsion. The bond angles and the molecule's three-dimensional form are determined by this arrangement. Moreover, ionization, which is the process of an atom gaining or losing electrons, can also be affected by electron-electron repulsion, as this can influence the energy necessary to detach an electron (**Table 10**).

Table 10: The pi atom, ionization and repulsion of electrons

PiAtom	Electron	Ionization	Repulsion
2	1	-11.160	11.134
40	2	-13.145	17.210
37	1	-14.120	12.340
4	1	-11.160	11.134
10	1	-14.120	12.340

In Chem3D, "d force" and "d length" relate to force and bond length (**Table 11**), respectively, in terms of molecular modelling and energy calculations. Chem3D utilizes these metrics to illustrate the energy effects arising from bond stretching, bending, and various interactions in a molecule, aiding in the assessment of its three-dimensional structure and stability.

Table 11: Predicted D force and D length for the synthesised pyrazole

Pi Bond	D Force	D Length
2-2	4.600	0.166
2-37	10.880	0.196
2-40	10.880	0.196

Pi Bond	D Force	D Length
2-4	7.790	0.156
37-40	10.880	0.196
4-10	10.880	0.290

Van der Waals (VDW) interactions can be expressed by a radius and an epsilon (ε) number (**Table 12**). The radius specifies the distance at which such interactions become significant, while the epsilon reflects the depth of the potential, indicating the strength of attraction. These factors are essential for modelling molecular behaviour and understanding how molecules interact.

Table 12: VDW interaction, radii and Epsilon values

VDW Interaction	Radius	Eps
2-23	0.400	2.340
1-5	0.046	3.340
6-23	0.600	1.830

From all the observed parameters the total energy for the synthesized 1H-Pyrazole carbonitrile derivatives are calculated below in the **(Table 13).**

Table 13: Total energy calculation for the synthesised Pyrazole

Factors	Energy
Stretch	36.1291
Bend	15.3207
Stretch-Bend	-2.1568
Torsion	21.1498
Non-1,4 VDW	7.5842
1,4 VDW	12.0519
Dipole/Dipole	4.2390
Total Energy	94.3178 l/mol

3.2.2. Impact on Biological Activity

The existence of the pyrazole nucleus in various structures enables a wide range of applications in fields such as technology, medicine, and agriculture. Generally, two nitrogen carrying pyrazole (amino azole) carbonitrile derivatives shows many biological significances i.e, antibacterial, anti-inflammatory, anti-fungal, anti-tubercular anti-microbial, anti-convulsant, anticancer, anti-viral, neuroprotective, angiotensin converting enzyme inhibitory and cholecystokinin-1 receptor antagonist32. Some of the pyrazole containing drugs include celecoxib, antipyrine, phenylbutazone, rimonabant and dipyrone which were already approved and in use nowadays33. Especially (E)-5-amino-3-styryl-1H-pyrazole-4-carbonitrile derivatives with the functional groups of amino and cyano groups in the pyrazole moiety could have applications in the agricultural field for crop protection. It can shield plants from a variety of diseases and pests. The synthesis and assessment of pyrazoles against various biological agents has been carried out by numerous research organizations. This study looks at recent research that links pyrazole structures to the corresponding drug discovery and antibacterial activity.

3.2.3. Molecular Docking

A quick, cost-effective, and advanced method for analysing experimental data and generating new ideas for molecular frameworks is computer-aided drug design. The rational drug discovery approach uses both structure-based and ligand-based drug design strategies as key tools. Docking studies are extensive computational techniques used in structure-based drug design to determine the optimal ligand-receptor interaction conformation and examine the relative orientation of the two through a system with a minimum amount of energy.

The pyrazole moiety serves as the fundamental structure for various functional groups, and its simplified method of synthesis, as well as potential uses, are expected to drive further chemical adaptation towards clinical applications. Because of their fascinating pharmacological effects, pyrazole complexes have recently received a lot of attention as biomolecules. This work aimed to perform an in silico analysis to propose a potent pharmacological drug based of 5 compounds produced from 1H-pyrazole carbonitrile. The affinity and interaction with these bacteria were investigated using molecular docking methods, and the binding conformation between the active ligand and the target was analysed with extra-precision by CB Dock molecular docking. The objective is to find more effective molecules against strains of Escherichia coli, Klebsiella oxytoca, Staphylococcus aureus, and Staphylococcus epidermidis with

Ligand((E)-5-amino-3-styryl-1H-pyrazole-4-carbonitrile (4a))-Protein (two proteins 4O9I and 2HI9) - docking.

3.2.3.1. Preparation of the protein

The crystal structures of two proteins, 4O9I (CHD4-Chromodomain-helicase-DNA-binding protein 4) and 2HI9 (Human Protein C inhibitor), are hydrolase inhibitors with 2.60 Å and 2.30 Å resolutions obtained from the Protein Data Bank (www.rcsb.org). These structures provide valuable insights into the mechanisms of action of these hydrolase inhibitors, highlighting their potential therapeutic applications in diseases where these proteins play a crucial role. The dual role of these proteins as both active participants and regulatory elements underscores their significance in preserving cellular balance and enabling vital biochemical reactions. Grasping these dynamics not only deepens our understanding of essential life processes but also paves the way for targeted therapeutic approaches to tackle various diseases associated with protein malfunctions. The intricate details of their binding sites and conformational changes will enhance the design of more effective inhibitors or modulators adapted to specific biological pathways. During synthesis, a number of processes ensured the protein was ready for docking. The crystal structure was first removed of all water molecules. Then, in order to correctly depict the protein's three-dimensional structure, the missing hydrogen atoms were inserted. The proteins were created using the Discovery Studio Visualiser. The active binding pocket where the ligands and the target interact was found using the integrated active site discovery algorithm in the Discovery Studio Visualise application.

3.2.3.2. Preparation of the Ligand and MD simulations

ChemDraw 12.0 software was used to construct the 2D structures of the compounds. Chem3D 12.0 was then used to transform all of the compounds from 2D to 3D structures and optimize them. Subsequently, AutoDock tools were used to store the molecules in PDBQT file format. The protein structure saved in the PDBQT file format, adjusted the Gasteiger charges, and added polar hydrogen using AutoDockTools. Then, using the open-source CB dock software, target compound (ligand)-protein docking was performed. To facilitate the use of the enzyme with a free active site during molecular docking, selected one of the two chains that comprised the enzyme and removed the ligand and water molecules. The next step is to prepare the grid. The grid plane should be in the middle, close to the binding site, and should be big enough to fit all residues that interact with the ligand and allow the ligand to rotate completely. The enzyme was then placed in the middle of the grid box, with as few grid points as possible in the X, Y, and Z directions. The second phase involved gathering the ligand library from the literature, utilizing AutoDock tools to convert the ligands'

2D structures to .pdb format, adding Gasteiger charges, fusing non-polar hydrogen, and identifying and defining rotational bonds. The CB dock was then used to complete the docking process. The final step involves analysing the docking results, focusing on the outcomes of the protein–ligand interaction simulation that yielded the most effective conformations with the highest binding energy (Figure 4 & Figure 5). Table 14 shows the binding sites, cavity volume, docking size, and vina score of the five cur pockets docking with the protein. The ligand-protein conformation with the lowest energy yielded the best docking result. The Vina score indicates the binding affinity between a ligand and a protein, while cavity volume refers to the size of the protein's binding pocket or cavity where a ligand is anticipated to attach. The volume of the cavity can greatly affect binding efficiency; a larger cavity can hold a range of ligands, whereas a smaller cavity may limit binding to particular molecules. Both the Vina score and cavity volume are essential for enhancing drug design and forecasting the interactions between ligands and their target protein receptors.

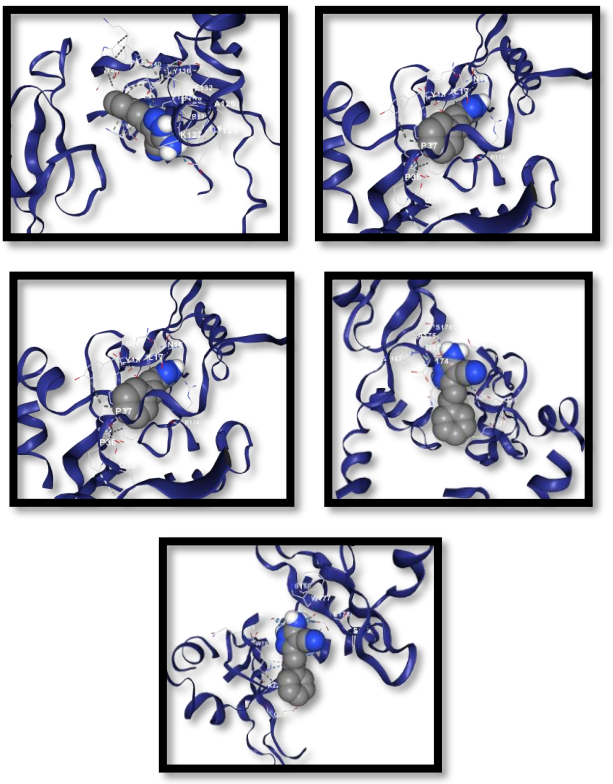

Figure 4: MD simulation, five curpockets & active site of the ligand 4a with the receptor 4O9I

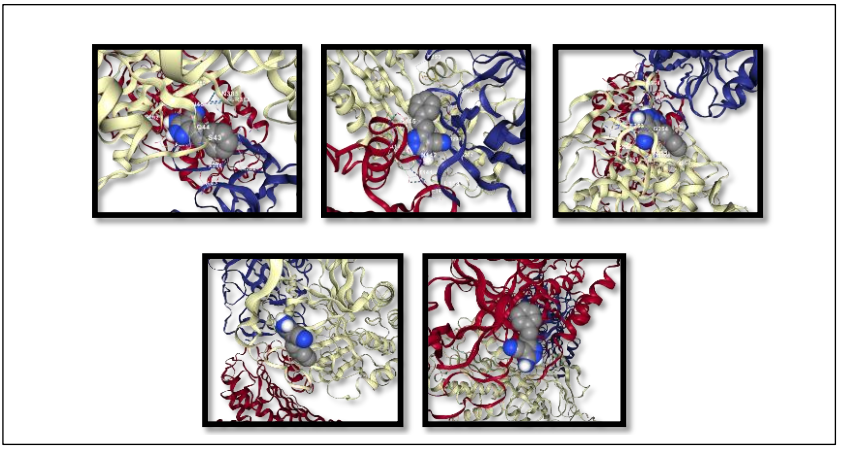

Figure 5: MD simulation, five curpockets & active site of the ligand 4a with the receptor 2HI9

The docking data shows that both 2HI9 and 4O9I have the largest cavity volume and the lowest Vina score, which means they attach to the target ligand, work as hydrolase inhibitors, and are involved in the antibacterial activities for drug development (**Table 14**).

Table 14: Vina score, Å^3 and docking size

4O9I

CurPocket ID	Vina score	Cavity volume (Å^3)	Center (x, y, z)	Docking size (x, y, z)
C1	-8.1	585	18, 7, 56	20, 20, 20
C4	-6.2	132	33, 13, 73	20, 20, 20

CurPocket ID	Vina score	Cavity volume (Å^3)	Center (x, y, z)	Docking size (x, y, z)
C2	-5.9	209	35, 26, 63	20, 20, 20
C3	-5.3	177	26, 1, 66	20, 20, 20
C5	-5.3	123	22, 8, 69	20, 20, 20

2HI9

CurPocket ID	Vina score	Cavity volume (Å)	Centre (x,y,z)	Docking size (x, y, z)
C1	-7.1	5120	1, 35, -85	35, 30, 35
C2	-7.1	4868	10, 19, -84	27, 35, 35
C5	-6.3	802	-4, 47, -89	20, 20, 20
C4	-6.0	1003	-14, 54, -66	26, 20, 20
C3	-5.5	1123	22, 37, -25	20, 28, 20

3.3. Antibacterial Activity

The agar well diffusion method was used to determine antibacterial activity. Nutrient agar is used to assess antibacterial activity. The strains were swabbed using sterile cotton swabs in the susceptible medium. The agar wells (5-mm diameter) were subsequently created in each of these plates using a sterile cork borer. Using sterilised dropping pipettes, several strains of Gram-positive and Gram-negative bacteria were added to the wells, and the plates were allowed to preincubate for one hour. After the plates were incubated for twenty-four hours at 37°C, the inhibitory zone was measured and reported[34].

Studies have shown that 1,3-diaryl pyrazole, pyrazole-derived aniline, and pyrazole-thiazole derivatives exhibit strong antibacterial activity against various gram-positive and gram-negative bacteria. By increasing cell membrane permeability, these compounds effectively penetrate bacterial cells and enhance their antibacterial effects. E. Coli, a gram-negative bacteria typically found in the lower intestines of warm-blooded creatures, which produce infections in the gut and the urinary tract. Klebsiella oxytoca an another gram negative bacteria which cause the infection in urinary tract and wounds[35]. The both gram negative bacterium was tested by disc diffusion technique using standard Amikacin 18 mm (AK 18) with dilution of 100 µL. The synthesized product shows the antibacterial activity against the both gram negative bacterium by 22mm and 12mm of zone of inhibition respectively (**Figure 6**). Especially E. Coli

shows the highest value of inhibition zone than that of Klebsiella oxytoca. Both Staphylococcus aureus and Staphylococcus epidermidis a gram positive bacterium which cause effects on the skin and skin-related tissues. It doesn't cause any effect on the healthy skin, but it produces several dangerous infections if it gets into the circulation or tissues within the body[36]. The synthesized compound **4a-e** shows the antibacterial activity of two gram positive bacterium shows maximum zone of inhibition than that of the MIC (Minimum Inhibitory Concentration) values. So, the synthesized product **4a-e** which was tested with micro-organisms in agar plate by disc diffusion method show high zone of inhibition and active against two gram positive and two gram negative bacterium. **Table 15** includes the synthetic compounds **4a-e** (ligands) that were evaluated with two positive and negative bacteria serve as Hydrolase inhibitors for drug discovery. The development of these pyrazole derivatives **4a-e** as antibacterial agents offers a promising avenue for addressing the growing concern of antibiotic resistance and exhibit unique mechanisms of action, distinct from existing antibiotics, making it challenging for bacteria to develop resistance. These compounds can disrupt bacterial cell membrane integrity, inhibit essential enzymes, or interfere with DNA replication, ultimately leading to bacterial growth inhibition or cell death. The broad-spectrum activity of pyrazole derivatives makes them promising candidates for the development of new antibacterial agents, particularly against Gram-negative bacteria like Escherichia coli, Klebsiella oxytoca, and Gram-positive bacteria such as Staphylococcus aureus and Staphylococcus epidermidis.

Figure 6: Antibacterial activities by Disk diffusion method

Table 15: Antibacterial activity of synthesized compound (4a)

Gram negative/Gram positive	Organisms	Standard disc	Zone of inhibition				
			4a	4b	4c	4d	4e

Gram negative	Echerichia Coli	AK- 18 mm	22 mm	20mm	22mm	25mm	24mm
Gram negative	Klebsiella oxytoca	AK -18 mm	15 mm	18mm	19mm	20mm	22mm
Gram positive	Staphylococcus aureus	AK- 18 mm	18 mm	17mm	21mm	20mm	24mm
Gram positive	Staphylococcus epidermidis	AK- 18 mm	19 mm	19mm	18mm	22mm	23mm

4. Conclusion

A facile Environmentally benign Tandem-Michael addition technique for the synthesis of (E)-5-amino-3-styryl-1H-pyrazole-4-carbonitrile derivatives using $AlCl_3$ as a catalyst in ethanol-water medium (an environmentally benign solvents) yields the product of 79 to 89% in 30 minutes have been developed and confirmed with the help of UV, FT-IR, ^{1}H and ^{13}C NMR techniques. This eco-friendly approach produces high yields and allows for a wide range of substrates with distinctive cinnamaldehydes. The products are then separated and purified by recrystallization using ethanol as a solvent. The ADME parameters of the synthesised drugs indicate their potential for oral absorption and central nervous system penetration. The complex network of both the proteins interaction is crucial for cellular functions, especially through the role of hydrolase inhibitors. Examining these interactions provides significant insights into the unique tasks that each protein performs inside the cell, shedding light on the intricate systems that influence biological activity. The synthesized 1H-pyrazole carbonitrile derivatives exhibit biological activity against Gram-negative bacteria like Escherichia coli, Klebsiella oxytoca, and Gram-positive bacteria such as Staphylococcus aureus and Staphylococcus epidermidis. Among the five, 4a has great responsiveness in antibacterial action, indicating a good possibility for creating novel therapies for resistant bacterial strains. And the next goal is to investigate its mechanisms of action and evaluate its effectiveness in therapeutic applications.

The use of pyrazole rings as scaffolds, which give additional binding sites, is unique in this work and suggests a viable route for future drug development. This work emphasises the usefulness of computational

approaches in speeding the identification of highly reactive compound 4a with superior pharmacokinetic features, and it promotes future development of pyrazole-based inhibitors.

Acknowledgement

We extend our sincere gratitude to the Tamil Nadu government for the scholarship that supported this research and facilitated its successful outcome.

Funding

No external funding was received for this work.

Contribution of Authors

Author 1 conceived the study, designed the research framework, collected and analyzed the data, and drafted the manuscript. The Corresponding author provided oversight and supervision for the whole work, refine the final document and reviewed the manuscript and supported author 1 in all the possible ways.

Conflict of Interest

The authors hereby declare no potential conflicts of interest with respect to the research, funding, authorship, and/or publication of this article

References

1. V.T. Kamble, K.R. Kadam, N.S. Joshi, D.B. Muley, HClO4–SiO2 as a novel and recyclable catalyst for the synthesis of bis-indolylmethanes and bis-indolylglycoconjugates, Catal. Commun. 2007, 8, 498.
2. Keshav Badhe * , Vijay Dabholkar and Swapnil Kurade, One-pot synthesis of 5-amino-1H-pyrazole-4-carbonitrile using calcined Mg-Fe hydrotalcite catalyst, Current Organocatalysis, 2018, 5, 3-12, doi, 10.2174/2213337205666180516094624.
3. Kalinski, C.; Lemoine, H.; Schmidt, J. Multicomponent reactions as a powerful tool for generic drug synthesis. Synthesis, 2008, 24, 4007-4011.
4. Ali A. Zwain1*, Sec. Biomaterials and Bio-Inspired Materials, Front. Mater, 2023, Volume 10 | https://doi.org/10.3389/fmats.2023.1196583
5. B Jiang; T Rajale; W Wever; SJ Tu; GG Li. Multicomponent reactions for the synthesis of heterocycles, Chem Asian J. 2010, 5(11), 2318-2335.

6. P Slobbe; E Ruijter; RVA Orru. Recent applications of multicomponent reactions in medicinal chemistry. Med Chem Commun. 2012, 3, 1189.

7. Little, R. D.; Masjedizadeh, M. R.; Wallquist, O.; McLoughlin, J. I. "The Intramolecular Michael Reaction". Org. React. 1995, 47, 315–552. doi:10.1002/0471264180.or047.02.

8. Lingjuan Zhang,a Xianxiu Xu,*a Qiu-rong Shao,b Ling Pana and Qun Liu*a , Tandem Michael addition/isocyanide insertion into the C–C bond: a novel access to 2-acylpyrroles and medium-ring fused pyrroles, Org. Biomol. Chem., 2013, 11, 7393-7399.

9. S. Safaei, I. Mohammadpoor-Baltork, A.R. Khosropour, M. Moghadam, S. Tangestaninejad, V. Mirkhani, R. Kia, Application of a multi-SO3H Brønsted acidic ionic liquid in water: a highly efficient and reusable catalyst for the regioselective and scaled-up synthesis of pyrazoles under mild conditions, RSC Adv. 2012, 2, 5610

10. Daidone, G.; Maggio, B.; Plescia, S.; Raffa, D.; Musiu, C.; Milia, C.; Perra, G.; Marongiu, E.M. Antimicrobial and antineoplastic activities of new 4-diazopyrazole derivatives. Eur. J. Med. Chem., 1998, 33, 375-382.

11. Tanitame, A.; Oyamada, Y.; Ofuji, K. Design, synthesis and structure–activity relationship studies of novel indazole analogues as DNA gyrase inhibitors with Gram-positive antibacterial activity. Bioorg. Med. Chem. Lett., 2004, 14, 2857-2862.

12. Bailey, M.D.; Hansen, E.P.; Hlavac, G.A.; Baizman, R.E.; Pearl, J.; Defelice, F.A.; Feigenson, E.M. 3,4-Diphenyl-1H-pyrazole-1- propanamine antidepressants. J. Med. Chem., 1985, 28, 256-260.

13. Gursoy, A.S.; Demirayak, G.; Capan, K. Synthesis and preliminary evaluation of new 5-pyrazolinone derivatives as analgesic agents. Eur. J. Med. Chem., 2000, 35, 359-364.

14. Allen, H.S.; Johns, A.B.; Gudmundsson, S.K.; Freeman, A.G. Synthesis of C-6 substituted pyrazolo[1,5-a]pyridines with potent activity against herpesviruses. Bioorg. Med. Chem., 2006, 14, 944- 954

15. G Brahmachari; B Banerjee, Catalyst-Free Organic Synthesis at Room Temperature in Aqueous and Non-Aqueous Media: An Emerging Field of Green Chemistry Practice and Sustainability, Current Green Chem. 2015, 2, 274-305.

16. V Srinivas; M Koketsu. Synthesis of indole-2-, 3-, or 5-substituted propargylamines via gold (III)-catalyzed three component reaction of aldehyde, alkyne, and amine in aqueous medium, Tetrahedron, 2013, 69, 8025-8033.

17. UMV Basavanag; AD Santos; LE Kaim; RG Montano; L Grimaud, Three-component metal-free arylation of isocyanides, Angew Chem Int Ed. 2013, 52, 7194- 7197.

18. AK Verma; SKR Kotla; D Choudhary; M Patel; RK Tiwari. Silver-catalyzed tandem synthesis of naphthyridines and thienopyridines via three-component reaction J Org Chem. 2013, 78, 4386-4401.

19. MS Singh; S Chowdhury, Recent developments in solvent-free multicomponent reactions: a perfect synergy for eco-compatible organic synthesis RSC Adv. 2012, 2, 4547-4592.

20. C Mukhopadhyay; PK Tapaswi; MGB Drew. Room temperature synthesis of tri-, tetrasubstituted imidazoles and bis-analogues by mercaptopropylsilica (MPS) in aqueous methanol: application to the synthesis of the drug trifenagrel, Tetrahedron Lett. 2010, 51, 3944-3950.

21. K Kumaravel; G Vasuki, Multi-component reactions in water, Curr Org Chem. 2009, 13, 1820-1841.

22. D Prasad; M Nath, Three-Component Domino Reaction in PPG: An Easy Access to 4-Thiazolidinone Derivatives, J Heterocycl Chem. 2012, 49, 628-633.

23. W Li; R Ruzi; K Ablajan; Z Ghalipt, One-pot synthesis of highly functionalized pyrano [2, 3-c] pyrazole-4, 4′-diacetate and 6-oxo-pyrano [2, 3-c] pyrazole derivatives catalyzed by urea, Tetrahedron. 2017, 73, 164-171.

24. G Brahmachari; B Banerjee, Facile and Chemically Sustainable One-Pot Synthesis of a Wide Array of Fused O- and N-Heterocycles Catalyzed by Trisodium Citrate Dihydrate under Ambient Conditions, Asian J Org Chem. 2016, 5, 271-286.

25. S Palle; J Vantikommu; R Redamala; M Khagga. J Applicable Chem. 2015, 4, 1190-1196.

26. P Mukherjee; S Paul; AR Das, Expeditious synthesis of functionalized tricyclic 4-spiro pyrano[2,3-c]pyrazoles in aqueous medium using dodecylbenzenesulphonic acid as a Brønsted acid–surfactant-combined catalyst, New J Chem. 2015, 39, 9480-9486.

27. A Saha; S Payra; S Banerjee, One-pot multicomponent synthesis of highly functionalized bio-active pyrano[2,3-c]pyrazole and benzylpyrazolyl coumarin derivatives using ZrO2 nanoparticles as a reusable catalyst, Green Chem. 2015, 17, 2859-2866.

28. KM Khan; MT Muhammad; I Khan; S Perveen; W Voelter, Rapid cesium fluoride-catalyzed Knoevenagel condensation for the synthesis of highly

functionalized 4,4'-(arylmethylene)bis(1H-pyrazol-5-ol) derivatives, Monatshefte fuer Chemie. 2015, 146, 1587- 1590.

29. P Gunasekaran; P Prasanna; S Perumal, L-Proline-catalyzed three-component domino reactions for the synthesis of highly functionalized pyrazolo [3, 4-b] pyridines, Tetrahedron Lett. 2014, 55, 329-332.
30. Maddila, S., Rana, S., Pagadala, R., Kankala, S., Maddila, S., & Jonnalagadda, S. B. (2015). Synthesis of pyrazole-4-carbonitrile derivatives in aqueous media with CuO/ZrO2 as recyclable catalyst. *Catalysis Communications*, *61*, 26–30. https://doi.org/10.1016/j.catcom.2014.12.005
31. M Srivastava; P Rai; J Singh; J Singh, Efficient iodine-catalyzed one pot synthesis of highly functionalised pyrazoles in water, New J Chem. 2014, 38, 302-307.
32. Silvana C. Plem, Diana M. Müller, Marcelo C. Murguía, Key Intermediates: A simple and Highly Selective Synthesis of 5-amino-1-aryl-1H-pyrazole-4-carbonitriles for Applications in the Crop Protection, Advances in Chemical Engineering and Science, 2015, 5, 239-261
33. Naim MJ, Alam O, Nawaz F, Alam MJ, Alam P. Current status of pyrazole and its biological activities. J Pharm Bioallied Sci. 2016, 8(1):2-17. doi: 10.4103/0975-7406.171694. PMID: 26957862; PMCID: PMC4766773.
34. Jéssica Venância Faria a b, Percilene Fazolin Vegi a, Ana Gabriella Carvalho Miguita c, Maurício Silva dos Santos c, Nubia Boechat b, Alice Maria Rolim Bernardino, Recently reported biological activities of pyrazole compounds, 2017, 25 (21), 5891-5903.
35. A.S. Shijila Rani, G. Senthilkumar, in Advances in Probiotics, 2021.
36. Tenaillon O, Skurnik D, Picard B, Denamur E, "The population genetics of commensal Escherichia coli". Nature Reviews. Microbiology, 2010, 8 (3): 207–17. doi:10.1038/nrmicro2298
37. Tracey A. Taylor; Chandrashekhar G. Unakal. Staphylococcus aureus Infection. StatPearls Publishing; 2024, https://www.ncbi.nlm.nih.gov/books/NBK441868/